Wellbore flow model for carbon dioxide and brine

Lehua Pan[1], Curtis M. Oldenburg[1], Yu-Shu Wu[2], and Karsten Pruess[1]

[1]***Lawrence Berkeley National Laboratory, Earth Sciences Division, 90-1116, Berkeley, CA 94720***
[2]***Colorado School of Mines, Petroleum Engineering, Golden, CO 80401***

Abstract

Wellbores have been identified as the most likely conduit for CO_2 and brine leakage from geologic carbon sequestration (GCS) sites, especially those in sedimentary basins with historical hydrocarbon production. In order to quantify the impacts of leakage of CO_2 and brine through wellbores, we have developed a wellbore simulator capable of describing non-isothermal open-well flow dynamics of CO_2-brine mixtures. The mass and thermal energy balance equations are solved numerically by a finite difference scheme with wellbore heat transmission handled semi-analytically. This new wellbore simulator can take as input the pressure, saturation, and composition conditions from reservoir simulators and calculate CO_2 and brine fluxes needed to assess impacts to vulnerable resources. This new capability is being incorporated into the Certification Framework (CF) developed for risk assessment of GCS sites.

Keywords: geologic carbon sequestration; well leakage, wellbore flow, risk assessment

1. Introduction

Wells are widely identified as likely pathways for CO_2 leakage through otherwise contiguous sealing formations overlying geologic carbon sequestration (GCS) reservoirs (e.g., [1]). Understanding the hazard of leaking wells in terms of quantifying CO_2 or brine fluxes that can be sustained by wells under various conditions is critical for risk assessment. In this study, we describe a wellbore flow simulator developed to model two-phase CO_2 and brine flow from large depths upward to the surface. The wellbore flow simulator will be used in the Certification Framework (CF) for evaluating CO_2 and brine leakage risk [2,3]. In this paper, we briefly discuss leakage processes in wells, present the equations and methods used in the new simulator, and present results of an example problem.

2. Modeled processes

The potential processes associated with CO_2 and brine leakage through wells include (1) well cement degradation by geochemical reactions, (2) geomechanical effects on cement fractures and cement bonding, (3) upward flow of CO2 and brine with transition from supercritical to gas phase, with (4) potential transition to liquid phase CO_2 depending on degree of Joule-Thomson cooling, (5) exsolution of CO_2 from the aqueous phase as pressure and temperature change, (6) heat transfer with the surrounding formation, and (7) cross-flow into or interaction with

layers of surrounding rock. If flow is occurring within degraded cement, it is likely that existing porous media flow simulators can model the CO_2 or brine leakage [4]. The focus of this work in on the upward (or downward) flow in the well occurring either in the tubing, within an annular region between casings, or between the casing and the rock, all of which fall into non-Darcy flow regimes. Regardless of the region in which flow is occurring, physical processes involving viscous or turbulent flow, phase change, and advective and conductive mass and heat transfer are relevant. In this work, we focus on two-phase flow of CO_2 and brine with non-isothermal effects and neglect well cement degradation and geomechanics.

3. Methods

3.1. Introduction

The approach we use for describing wellbore flow is based on the drift-flux model (DFM) [5] for transient two-phase non-isothermal flow of CO_2-water mixtures. Conservation equations for mass, momentum and energy under different flow regimes in the wellbore are solved numerically while wellbore heat transmission is handled semi-analytically. We implement the DFM in TOUGH2 [6] with the ECO2N equation of state module [7]. The conventional approach for calculating the mixture velocity in the drift-flux model (DFM) is often based on the steady-state pressure loss equation for wellbore flow [8]. To improve simulation performance in well-bore flow processes involving high fluxes, we have extended the DFM to include the transient terms of the momentum conservation equations in calculating the velocity from the pressure gradient.

3.2. Mass and Energy Conservation

According to mass and energy conservation principles, the generalized conservation equation of mass components and energy in the wellbore can be written as

$$\frac{\partial M^{\kappa}}{\partial t} = q^{\kappa} + F^{\kappa} \tag{1}$$

where superscript κ is the index for the components, κ = 1 (H_2O), 2 (CO_2), and 3 (energy, taken as internal and kinetic energy here), M^{κ} are the accumulation terms of the components κ; q^{κ} are external source/sink terms for mass or energy components; and F^{κ} are the mass or energy transport terms along the borehole due to advective processes. Note in this development we refer to H_2O and CO_2 components, but the treatment of components is general and our implementation includes CO_2, H_2O, and NaCl to model CO_2 and brine. Note further that we refer to liquid and gas phases, but the gas phase includes both true gas and supercritical forms of CO_2 depending on pressure and temperature.

3.3. Accumulation Terms

The accumulation term (M^{κ}) of Eq. 1 for the mass components (H_2O and CO_2) in single- or two-phase system is given by

$$M^{\kappa} = \rho_G S_G X_G^{\kappa} + \rho_L S_L X_L^{\kappa} \quad (\kappa = 1 \text{ and } 2) \tag{2}$$

where X_{β}^{κ} is the mass fraction of component κ in fluid phase β (β = G for gas; β = L for liquid), ρ_{β} is the density of phase β; and S_{β} is the local saturation of phase β defined as

$$S_G = \frac{A_G}{A} = \frac{A_G}{A_G + A_L} \tag{3}$$

where A is the well cross-sectional area, and A_G and A_L denote the cross-sectional areas occupied by gas and liquid over the cross section at a given distance along the well. The accumulation term for energy is defined as

$$M^3 = \sum_{\beta} \left(\rho_\beta S_\beta U_\beta + \frac{1}{2} \rho_\beta S_\beta u_\beta^2 \right) \tag{4}$$

where U_β is the internal energy of phase β, and u_β is the average phase velocity in the wellbore. The two right-hand-side terms in Eq. 4 represent the accumulation of internal and kinetic energy, respectively.

3.4. Flow Terms

Transport along the wellbore is governed in general by processes of advection, diffusion, and dispersion, and is also subject to other processes such as exchanges with the formation at feed zones. The total advective mass transport term for component κ can be written in one-dimension as

$$F^\kappa = -\left[\frac{\partial\left(\rho_G X_G^\kappa \mathrm{u}_G\right)}{\partial z} + \frac{\partial\left(\rho_L X_L^\kappa \mathrm{u}_L\right)}{\partial z} \right] \tag{5}$$

where u_β is the average velocity vector of phase β within the wellbore, and z is the along-wellbore (typically vertical) coordinate.

The transport terms for energy in the wellbore include those due to (1) advection, (2) kinetic energy, (3) potential energy, and (4) lateral wellbore heat loss/gain. The overall one-dimensional energy transport term can be written as

$$F^3 = -\sum_{\beta} \left[\frac{\partial}{\partial z}\left(h_\beta \rho_\beta S_\beta \mathrm{u}_\beta\right) + \frac{\partial}{\partial z}\left(\frac{1}{2} \rho_\beta S_\beta u_\beta^2\right) - \rho_\beta S_\beta u_\beta g \right] - q'' \tag{6}$$

where h_β is specific enthalpy of fluid phase β, g is the gravitational acceleration, and q'' is the wellbore heat loss/gain per unit length of wellbore.

3.5. Momentum Conservation Using the Drift-Flux Model (DFM)

In order to model the advective transport terms (F_β and u_β), we invoke the DFM [9, 5] to describe both single-phase and multiphase flow in wellbores. The basic idea of the DFM is to consider the two-phase liquid-gas mixture as a single effective fluid phase with slip between gas and liquid arising from non-uniform velocity profiles, as well as from buoyancy forces accounted for by empirically relating phase fractions and velocities to the mixture velocity.

The gas velocity u_G is related to the mixture velocity u as

$$u_G = C_0 u + u_d \tag{7}$$

where C_0 is the profile parameter (or distribution coefficient), and u_d is the drift velocity of the gas describing the buoyancy effect [5], where

$$u_d = \frac{\left(1 - C_0 S_G\right) C_0 u_c K_u}{C_0 S_G \sqrt{\rho_G / \rho_L} + 1 - C_0 S_G} \tag{8}$$

where K_u is the Kutateladze number and u_c is the "characteristic velocity," a measure of the velocity of bubble rise in a liquid column. Bubble rise is given by

$$u_c = \left[\frac{g \sigma_{GL} \left(\rho_L - \rho_G\right)}{\rho_L^2} \right]^{1/4} \tag{9}$$

where σ_{GL} is the surface tension between gas and liquid phases. By definition, the average mixture velocity (u) is the volumetrically weighted velocity

$$u = S_G u_G + (1 - S_G) u_L \tag{10}$$

Therefore, the liquid velocity can be determined as

$$u_L = \left(\frac{1 - S_G C_0)}{1 - S_G}\right) u - \left(\frac{S_G}{1 - S_G}\right) u_d \qquad (11).$$

The profile parameter C_0 varies from 1.0 to 1.2 and is assumed to be a smooth function of gas saturation:

$$C_0 = \begin{cases} 1.2 & S_G < S_1 \\ 1 + 0.1\left[1 + \cos\left(\pi \dfrac{S_G - S_1}{S_2 - S_1}\right)\right] & S_1 \le S_G \le S_2 \\ 1.0 & S_G > S_2 \end{cases} \qquad (12)$$

with the two turning saturations, S_1 and S_2, set at 0.8 and 0.9999, respectively.

To calculate the mixture velocity, we use the transient momentum conservation equation with the steady-state assumption about the wall shear stress. Specifically, we start from the transient momentum equation

$$\frac{\partial}{\partial t}(\rho u) + \frac{\partial}{\partial L}(\rho u^2) = -\frac{\partial P}{\partial L} - \frac{f \rho u^2}{4 r_w} - \rho g \cos\theta \qquad (13)$$

where u is the mixture velocity in the wellbore, L is a length of the wellbore section (positive upward), ρ is the mixture density and θ is the local angle between wellbore section and the vertical direction. The friction coefficient (f) is a function of the Reynolds number (Re) for laminar and turbulent flows by

$$f = \frac{64}{\mathrm{Re}} \text{ for Re < 2400, and } \frac{1}{\sqrt{f}} = -2\log\left[\frac{2\varepsilon/d}{3.7} - \frac{5.02}{\mathrm{Re}}\log\left(\frac{2\varepsilon/d}{3.7} + \frac{13}{\mathrm{Re}}\right)\right] \text{ for Re > 2400} \qquad (14)$$

where the Reynolds number is defined as $Re = \rho u d/\mu$ where μ is the mixture viscosity.

The fundamental challenge of implementing the transient DFM is in handling the coupling between friction factor and velocity. The first-order approach is to use a velocity from the prior time step to calculate the friction factor for the current time step. Our experience with this approach produced unsatisfactorily small time-step sizes, and motivated us to use a different approach as described below.

3.6. Solving the Discretized Equations

In the framework of TOUGH2, the mass and energy flux terms are calculated at each Newtonian iteration from the most recently updated primary variables (usually pressure, mass fractions, and temperature). Within the wellbore at each iteration, we calculate the mixture velocity (Eq. 10) first, and then calculate the gas velocity (Eqs. 10-11). As for marching in time, the momentum conservation equation (Eq. 13) is solved semi-explicitly as

$$u^{n+1} = \frac{DR^{n+1} + \dfrac{1}{\Delta t}\rho^n u^n - \left(\dfrac{\partial \rho u^2}{\partial L}\right)^n}{\dfrac{\rho^n}{\Delta t} + \dfrac{f^n \rho^n u^n}{4 r_w}} \qquad (15)$$

where, the superscript n and n+1 indicate the previous and current time levels, respectively; Δt is the time-step size, and DR is the total driving force given by

$$DR = -\frac{\partial P}{\partial L} - \rho g \cos\theta \qquad (16).$$

Normally, the pressure gradient caused by elevation change contributes from 80 to 95% of the total pressure gradient and the friction loss represents 5 to 20%, whereas the acceleration component is normally negligible and can become significant only if a compressible phase exists at relatively low pressures [8]. Therefore, the solution of Eq. 15 is more like an implicit formulation considering the above-normal pressure gradient components.

When the system reaches steady state there is no mass accumulation, thus Eq. 13 reduces to the pressure loss equation [8] given by

$$-\frac{dP}{dL} = \frac{f\,\rho\,u^2}{4r_w} + \rho\,u\frac{du}{dL} + \rho\,g\cos\theta \qquad (17).$$

The component mass- and energy-balance equations of Eq. (1) are discretized in space using the conventional integral finite-difference scheme of TOUGH2 for the 1-D wellbore system. Apart from the special treatment of the momentum equation (Eq. 15), time discretization is carried out using a backward, first-order, fully implicit finite-difference scheme. The discrete nonlinear equations for H_2O, CO_2, NaCl, and energy conservation at node i (well block) can be written in a general form as

$$\left[M_i^{\kappa,n+1} - M_i^{\kappa,n}\right]\frac{V_i}{\Delta t} = F_{i,i+1/2}^{\kappa,n+1} - F_{i,i-1/2}^{\kappa,n+1} + Q_i^{\kappa,n+1} \quad (\mathrm{i} = 1, 2, 3, \ldots, N) \qquad (18)$$

where superscript n denotes the previous time level, with n+1 the current time level to be solved, subscript i refers to the index of N wellbore gridblocks, Δt is time-step size, V_i is the volume of wellbore node i (wellbore diameter may vary). The flow terms in Eq. 18 are generic and include mass fluxes as well as heat transfer. The mass flow term is given by

$$\mathrm{F}_{ij}^{\kappa} = A_{ij}\sum_{\beta}\left(\rho_\beta X_\beta^{\kappa}\right)_{ij+1/2} u_{\beta,ij} \qquad (19)$$

The total heat flux along the connection of nodes i and j, including advective and radial heat conduction terms, may be evaluated by

$$F_{\mathrm{ij}}^{3} = \sum_{\beta}\left[\left(\rho_\beta h_\beta\right)_{ij+1/2} u_{\beta,ij}\right] \qquad (20)$$

and heat loss/gain by lateral wellbore heat transmission is given by

$$Q_{\mathrm{i}}^{3} = -A_{wi}\left(K_{wi}\right)\left[\frac{T_i - T_\infty(z)}{f(t)}\right] \qquad (21)$$

where A_{wi} is the lateral area between wellbore and surrounding formation, K_{wi} is thermal conductivity (or overall heat transfer coefficient) of wellbore/formation, $T_\infty(z)$ is ambient temperature, and $f(t)$ is the Ramey's well heat loss function.

In evaluating the flow terms in Eqs. 19 and 20, subscript ij + 1/2 is used to denote a proper averaging or weighting of advective mass transport or heat transfer properties at the interface or along the connection between two blocks or nodes i and j ($j = i - 1$ or $i + 1$). In addition, fully upstream weighting should be used in Eqs. 19 and 20 for numerical stability. The mass or energy sink/source in Eq. 18 at node i, Q_i^{κ}, is defined as the mass or energy exchange rate per time and can be used for interaction with feed zones in the well.

The standard TOUGH2 fully implicit residual-based method is used to solve the discrete nonlinear equations using Newton iteration. In general, we need to solve for four primary variables (pressure, saturation or mass fractions of H_2O or CO_2 in fluids depending on phase conditions, mass fraction of NaCl, and temperature) per node. The remaining variables such as viscosities, densities, thermal conductivities, etc. are secondary variables that can be calculated from selected primary variables. The Newton iteration process continues until the residuals are reduced below preset convergence levels. The sparse Jacobian matrices arising in Newton's method are solved by conjugate gradient or direct linear equation solvers provided in TOUGH2.

4. Verification

To verify the well-bore flow solution approach, we simulated a case of isothermal steady-state single-phase water flowing up the wellbore at 25 ^{o}C at a rate of approximately 2 kg/s and compared the result with the theoretical pressure profile along the well from the steady-state pressure loss equation (Eq. 17). A sketch of the model system used for this verification problem (and for the test problem that follows) is shown in Figure 1a. In the verification problem, we increased the pressure at the bottom boundary slightly above hydrostatic and ran the model to steady state under isothermal conditions (T = 25 ^{o}C). The differences in pressure in the well between the flowing steady-state result and the initial hydrostatic condition calculated in the simulation are of order 0.1%. Shown in Figure 1b are the theoretical (Eq. 17) and calculated pressures along the wellbore, along with the relative error. As shown in Figure 1b, the relative error between the theoretical and calculated pressures is negligibly small. This verification problem confirms the ability of the code to solve a steady-state single-phase flow up the well.

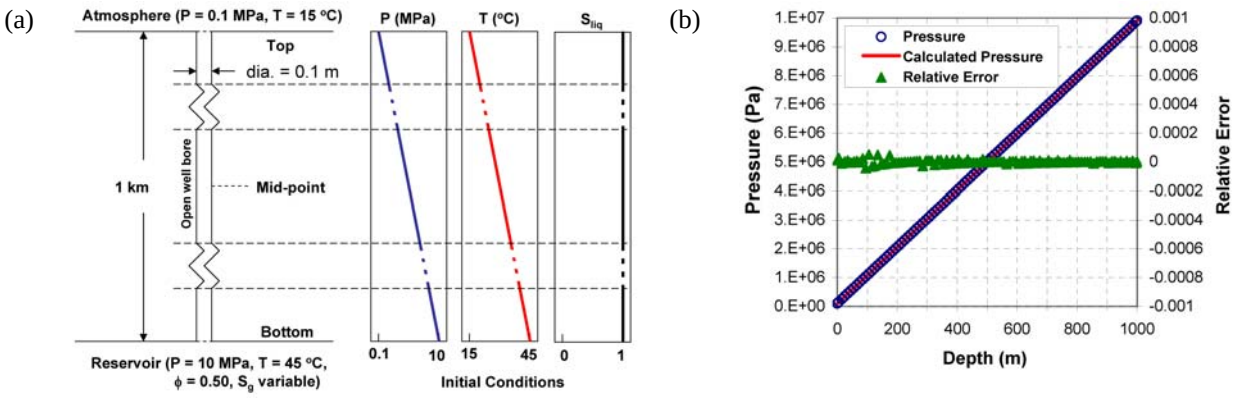

Figure 1. (a) Schematic of the wellbore flow problem with initial conditions. (b) Results of verification problem comparing theoretical pressure and pressure calculated using well-bore flow simulator along with relative error for single-phase liquid flow up the well bore at ~2 kg/s (note this verification problem was isothermal at 25 ^{o}C).

5. Example leakage problem

To demonstrate the capabilities of the new wellbore flow model, we present results for a case of two-phase flow up an open wellbore. The system initial conditions are hydrostatic pressure, temperature varying linearly top-bottom from 15-45 ^{o}C, and 100% water in the well as shown in Figure 1a. Starting from hydrostatic conditions in the well, an overpressure of 0.1 MPa (1 bar) is applied to the reservoir to mimic an injection-induced overpressure. The scenario envisioned is that of the tip of a migrating CO_2 plume at 10% gas saturation encountering an open well initially filled with water. Note that unlike other conditions in CO_2-brine systems [10], this problem results in a steady-state non-oscillatory flow which we chose for simplicity in testing the model.

With reference to Figure 2, we observe in this test problem the early-time upward flow of water within the well at all depths as driven by the 0.1 MPa pressure perturbation at the bottom. Gas flow does not begin until approximately t = 20 s when gas appears at the bottom of the well. By t ~ 500 s, gas flows at the middle and top of the well. The flow rate of CO_2 reaches approximately 1.4 kg/s in this open wellbore case.

Further insight into the processes modeled can be obtained from Figure 3 which shows gas saturation, gas density, pressure, and temperature throughout the well as a function of time. As shown, the well is initially filled with water and gas progressively fills the well from the bottom up. After 30 minutes (1800 s), gas is fairly evenly distributed throughout the well from 10% at the bottom to nearly all gas at the top. The reasons for this increase in gas saturation are (1) the exsolution of gas from the liquid as pressure drops and (2) the large expansion that CO_2 undergoes as it transitions from supercritical to gaseous conditions. This transition occurs around the critical

pressure of 7.4 MPa (74 bar), at a depth of approximately 800 m. The gas density plot in Figure 3 shows the sharp decrease in gas density at depths around 800 m. Temperature also affects CO_2 solubility, but temperature becomes relatively constant as steady flow develops, resulting in decreasing CO_2 mass fractions being controlled mostly by pressure. The temperature contour shows the evolution from a conductive profile controlled by the geothermal gradient to an advective profile controlled by upward fluid flow. In between the initial and steady states, there are some local maxima and minima arising from expansion and dissolution of CO_2 as gas phase rises upwards.

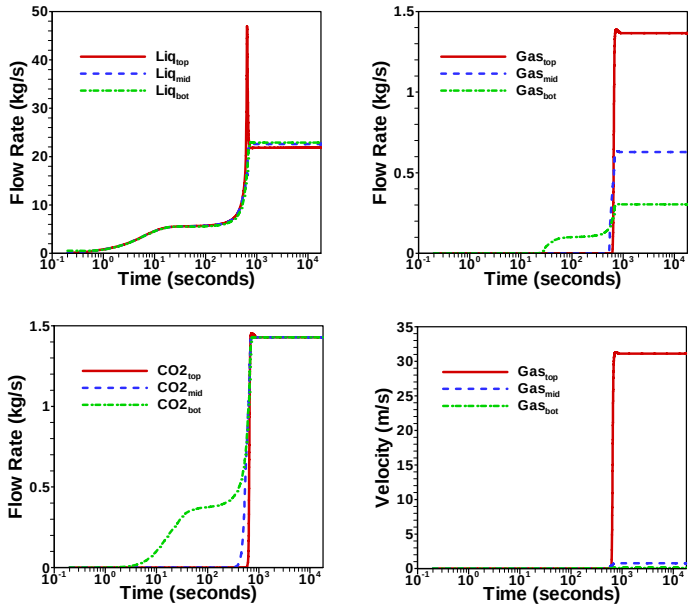

Figure 2. Flow rates and velocities of CO_2 and water at three levels in the well (bottom, middle, and top).

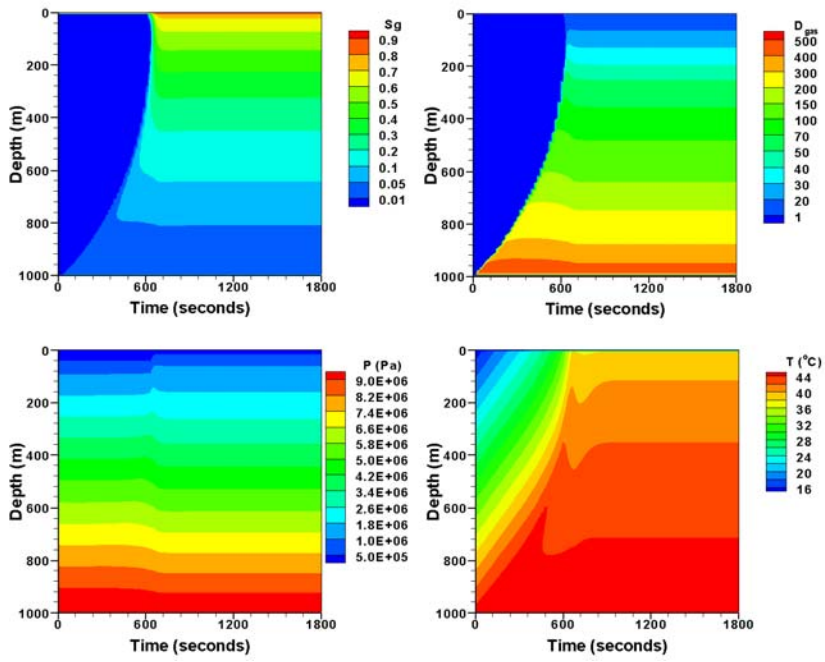

Figure 3. Profiles of .gas saturation, gas density, pressure, and temperature in the wellbore as a function of time.

6. Conclusions

We have developed a well-bore flow simulator that models two-phase CO_2-brine mixtures for use in GCS leakage studies. This simulation capability is intended to be used for quantifying potential leakage up wells using pressures and CO_2 saturations at depth calculated by reservoir simulation. Although the test problem is based on flow up an open borehole, the approach can be used for flow in an annulus region by suitable modifications of roughness coefficients and geometric parameters. The fundamental elements of advection, diffusion, and phase change are independent of the particular flow geometry. Similarly, the approach can be applied to non-vertical and horizontal wells with the caveat that flow in the well is always one-dimensional. Finally, the wellbore simulator can be used for downward flow, e.g., injection calculations to determine bottom-hole pressure for given flow rates to avoid exceeding formation fracture pressure.

7. Acknowledgments

We thank Scott Imbus (Chevron) for support and encouragement. This work was supported in part by the CO_2 Capture Project (CCP) of the Joint Industry Program (JIP), and by Lawrence Berkeley National Laboratory under U.S. Department of Energy Contract No. DE-AC02-05CH11231.

8. References

1. Gasda, S.E., S. Bachu, and M.A. Celia, The potential for CO_2 leakage from storage sites in geological media: Analysis of well distribution in mature sedimentary basins, *Env. Geol. 46*(6-7), 707-720, 2004.

2. Oldenburg, C.M., and S.L. Bryant, Certification Framework for Geologic CO_2 Storage, Sixth Annual Conference on Carbon Capture and Sequestration, National Energy Technology Laboratory, Pittsburgh, PA, May 7-10, 2007.

3. Oldenburg, C.M., J.-P. Nicot, and S.L. Bryant, Case studies of the application of the Certification Framework to two geologic carbon sequestration sites, Energy Procedia, this volume, 2009.

4. Nordbotten, J.M., M.A. Celia, and S. Bachu, Analytical solutions for leakage rates through abandoned wells, Water Resour. Res. 40:W04204, 2004.

5. Shi, H., J.A. Holmes, L.J. Durlofsky, K. Aziz, L.R. Diaz, B. Alkaya, and G. Oddie, Drift-flux modeling of two-phase flow in wellbores, Soc. Pet. Eng. J., 24-33, 2005.

6. Pruess, K., C.M. Oldenburg and G.J. Moridis. TOUGH2 User's Guide Version 2. E. O. Lawrence Berkeley National Laboratory Report LBNL-43134, November 1999.

7. Pruess, K., and N. Spycher, ECO2N – A fluid property module for the TOUGH2 code for studies of CO_2 storage in saline formations, Energy Conversion and Management 48, 1761-1767, 2007.

8. Brill and Mukherjee, Multiphase Flow in Wells. Monograph Volume 17, SPE Henry L. Doherty Series. 1999.

9. Zuber, N., and J.A. Findlay, Average volumetric concentration in two-phase flow systems, J. Heat Transfer ASME, 87(4), 453-468, 1965.

10. Pruess, K. On CO_2 Fluid Flow and Heat Transfer Behavior in the Subsurface, Following Leakage from a Geologic Storage Reservoir, *Env. Geol.,* Vol. 54, No. 8, pp. 1677–1686, June 2008.